

Effect of Hydrophobe Content on Intra- and Interpolymer Self-Associations of Hydrophobically Modified Poly(sodium 2-(acrylamido)-2-methylpropanesulfonate) in Water

Hiroshi Yamamoto and Yotaro Morishima*

Department of Macromolecular Science, Graduate School of Science, Osaka University, Toyonaka, Osaka 560-0043, Japan

Received May 18, 1999; Revised Manuscript Received August 16, 1999

ABSTRACT: As an extension of our previous fluorescence studies of random terpolymers of sodium 2-(acrylamido)-2-methylpropanesulfonate (AMPS), *N*-dodecylmethacrylamide (DodMAM), and 1 mol % *N*-(1-naphthylmethyl)methacrylamide (fluorescence label), intra- and interpolymer self-associations of these polymers in aqueous solution were investigated by ¹H NMR relaxation, fluorescence depolarization, and quasielastic light scattering (QELS) methods. These studies were conducted with a focus on the effect of the DodMAM content (f_{Dod}) on the association behavior of these polymers over the f_{Dod} range of 10–60 mol %. At $f_{\text{Dod}} = 10$ mol %, the polymer-bound dodecyl groups undergo mostly intrapolymer association, but a small fraction of the hydrophobes undergo interpolymer association, QELS showing a bimodal distribution as the polymer concentration is increased. In the range $10 < f_{\text{Dod}} \leq 50$ mol %, however, QELS data indicated a strong preference for intrapolymer associations independent of the polymer concentration, leading to the formation of unimolecular micelles (unimer micelles). QELS data suggested that unimer micelles with a relatively loose conformation (a second-order structure) formed at $f_{\text{Dod}} < 30$ mol % collapse into a highly compact unimer micelle with a third-order structure at an f_{Dod} between 30 and 40 mol % upon an increase in f_{Dod} . The most compact unimer micelle was found to be formed at $f_{\text{Dod}} = 50$ mol % whose hydrodynamic radius (R_h) was about 5 nm (in 0.05 M NaCl). When f_{Dod} is increased beyond 50 mol %, however, interpolymer associations abruptly occur. Multipolymer aggregates thus formed show unimodal distributions with a narrow width in the QELS relaxation times independent of polymer concentration whereas R_h increases with increasing polymer concentration (e.g., $R_h = 15$ nm in 0.05 M NaCl at $f_{\text{Dod}} = 60$ mol %). Thus, this interpolymer association at $f_{\text{Dod}} > 50$ mol % is very different from that at $f_{\text{Dod}} < 10$ mol %. The structure of this rather unusual multipolymer aggregate at $f_{\text{Dod}} > 50$ mol % remains an open question.

Introduction

There has been growing interest in the self-association phenomena of hydrophobically modified water-soluble polymers in the past decades. This is in part because of their biological relevance and in part because of their usefulness for such industrial applications as paints, coatings, cosmetics, inks, foodstuff, and drugs.^{1–5}

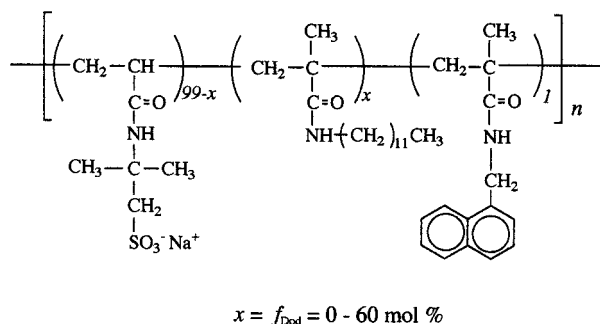
The self-association of hydrophobes covalently linked to water-soluble polymers can occur either within a single polymer chain or among different polymer chains, or both. In highly dilute aqueous solutions, in general, intrapolymer hydrophobe association may be favorable, but with an increase in the polymer concentration, interpolymer hydrophobe association tends to occur. Thus, polymers with a strong tendency for interpolymer associations lead to a large increase in solution viscosity or gelation or precipitation upon an increase in the polymer concentration. In contrast, polymers with a strong propensity for intrapolymer self-association may lead to the formation of unimolecular micelles (unimer micelles) independent of polymer concentration.

The sequence distribution of hydrophilic and hydrophobic monomer units in amphiphilic copolymers is a particularly important structural factor that influences whether the hydrophobe association occurs in an intra- or interpolymer fashion. Chang and McCormick⁶ have demonstrated that even a subtle difference in the sequence distribution in amphiphilic random copolymers has a significant effect on the association behavior of polymer-bound hydrophobes. Blocky sequences of

hydrophobic monomer units have a strong tendency for interpolymer association, whereas random and alternating sequences have a tendency for intrapolymer association.^{7–13} Furthermore, amide spacer bonds between hydrophobes and the polymer main chain seem to be a structural factor that favors intrapolymer hydrophobe associations. Hydrogen bonding between the adjacent amide spacers may be responsible for the preference of intrapolymer hydrophobe associations.^{14–16}

We previously reported that copolymers of sodium 2-(acrylamido)-2-methylpropanesulfonate (AMPS) and *N*-dodecylmethacrylamide (DodMAM) showed a strong tendency for intrapolymer associations and that the copolymers form unimer micelles when the content of the dodecyl groups in the copolymer is sufficiently high.^{14–16} In these copolymers, AMPS and DodMAM units are randomly distributed along a polymer chain, as indicated by the monomer reactivity ratios,¹⁷ and dodecyl moieties are linked to the main chain via amide spacer bonds. In an earlier work,¹⁸ we investigated the self-association of AMPS–DodMAM copolymers (with pyrene and/or naphthalene labeled) by fluorescence and viscometric techniques as a function of the DodMAM content (f_{Dod}) in the copolymer. Results from the previous study suggested that the intrapolymer association of dodecyl groups occurred when $f_{\text{Dod}} \geq 10$ mol % in 0.1 M NaCl aqueous solutions, resulting in a significant decrease in the conformational size.¹⁸ Although viscosity data showed no further contraction of the polymer chains at $f_{\text{Dod}} \geq 20$ mol % upon an increase in f_{Dod} , fluorescence data indicated a considerable increase in

Chart 1



the compactness of the polymer chains at $f_{\text{Dod}} \geq 20 \text{ mol } \%$. This is because fluorescence provides microscopic information on hydrophobe associations and conformational changes in hydrophobically modified polymers whereas viscosity reports only a change in a global conformation.

In the present study, we further characterized the self-associating behavior of the same type of AMPS–DodMAM copolymers of a wider range of f_{Dod} (0–60 mol %) using ^1H NMR relaxation, fluorescence depolarization, and quasielastic light scattering (QELS) techniques. For a fluorescence depolarization study, the polymers were labeled with naphthalene (1 mol %) by terpolymerization of the three corresponding monomers (Chart 1). On the basis of experimental results, we propose hypothetical models for unimer micelles with a second-order and third-order structure depending on f_{Dod} .

Experimental Section

Monomers. *N*-Dodecylmethacrylamide (DodMAM) and *N*-(1-naphthylmethyl)methacrylamide (1NpMAM) were prepared as reported previously.^{19,20} 2-(Acrylamido)-2-methylpropanesulfonic acid (AMPS) was purchased from Wako Pure Chemicals and used without further purification. 2,2'-Azobis(isobutyronitrile) (AIBN) (Wako Pure Chemicals) was recrystallized twice from ethanol prior to use.

Polymers. The naphthalene-labeled polymers were prepared by terpolymerization of AMPS, DodMAM (0, 10, 20, 30, 40, 50, 55, or 60 mol %), and *N*-(1-naphthylmethyl)methacrylamide (1 mol %) in the presence of AIBN in *N,N*-dimethylformamide at 60 °C. The details of the polymerization procedures were reported elsewhere.¹⁵ The polymers were purified by reprecipitations from methanol into excess ether, and then polymer solutions in a dilute aqueous NaOH were dialyzed against pure water for a week. The compositions of the terpolymers were determined by N/C ratios from elemental analysis and UV absorbances. Apparent molecular weights for all the polymers, estimated by GPC (see below), are in the range $(1.5\text{--}3.0) \times 10^4$ (weight-average), and there was no particular dependence of the molecular weight on the content of the DodMAM unit in the copolymer. The copolymerization of AMPS and DodMAM is an "ideal copolymerization", leading to copolymer compositions equal to monomer feed compositions and completely random distributions of the monomer sequences.¹⁷

Other Materials. *n*-Dodecyl hexaoxyethylene glycol monoether (C_{12}E_6) was used as supplied by Nikko Chemical Co. Sodium chloride was purchased from Wako Pure Chemicals and was used without further purification. Milli-Q water was used for all measurements.

Measurements. (a) GPC. Measurements were performed at 40 °C with a JASCO GPC-900 equipped with Shodex Asahipak GF-7M HQ columns in combination with a JASCO UV-975 detector. A 0.2 M lithium perchlorate solution in methanol (HPLC grade purchased from Wako Pure Chemicals) was used as an eluent at a flow rate of 1 mL/min. Molecular

weights of the polymer samples were calibrated with poly(ethylene oxide) standard samples purchased from Scientific Polymer Products.

(b) ^1H NMR Relaxation Times. ^1H NMR spectra were recorded with a JEOL EX-270 and a GSX-400 spectrometer using a deuterium lock at a constant temperature of 30 °C during the whole run. Sample solutions of 1.0 mg/mL polymer in D_2O containing 0.05 M NaCl were deaerated in NMR tubes by purging with Ar gas for 30 min prior to measurement. The resonance due to impurity water in the D_2O solutions was decoupled. Proton spin–lattice relaxation times (T_1) were determined using a conventional inversion–recovery technique with a $180^\circ\text{--}\tau\text{--}90^\circ$ pulse sequence.^{21–23} Proton spin–spin relaxation times (T_2) were determined by the Carr–Purcell–Meiboom–Gill (CPMG) method using a $\{90^\circ_x\tau(180^\circ_y2\tau)_n\}$ pulse sequence.²⁴

(c) Fluorescence Depolarization. Polarized steady-state fluorescence intensities for the naphthalene-labeled polymers were recorded on a Hitachi F-4500 fluorescence spectrophotometer equipped with a polarizer and analyzer on the excitation and detection sides, respectively. The fluorescence anisotropy (r) was calculated from

$$r = (I_{\text{vv}} - gI_{\text{vh}})/(I_{\text{vv}} + 2gI_{\text{vh}}) \quad (1)$$

where h and v denote the horizontal and vertical orientations of the excitation and emission polarizers, respectively, and g is a factor for the instrumental correction (i.e., $g = I_{\text{hv}}/I_{\text{hh}}$). The rotational correlation time (τ_ϕ) was calculated from²⁵

$$r_0/r = 1 + 3\tau/\tau_\phi \quad (2)$$

where r_0 is the limiting value of r for steady-state fluorescence in rigid media where no rotation occurs, and τ is the fluorescence lifetime. The value of r for 1NpMAM in glycerol measured at 265 K (i.e., $r = 0.18$) was used as a value for r_0 . The justice of this value was confirmed by time-resolved fluorescence depolarization measurement.

(d) Quasielastic Light Scattering (QELS). QELS data were obtained using an Otsuka Electronics Photol DLS-7000 light scattering spectrometer equipped with a 75 mW Ar laser lamp and detector optics. An ALV-5000E digital multiple- τ correlator (Langen-GmbH) was employed for data collection. The autocorrelation function was measured at different angles ($50^\circ\text{--}150^\circ$) at 25 °C. Sample solutions of the polymers were prepared by dissolving solid polymer samples (recovered by a freeze-drying technique) in water containing 0.05 M NaCl. The solutions were heated at 90 °C for 15 min with vigorous stirring. Sample solutions were filtered with a 0.2 μm pore size membrane filter prior to measurement.

The intensity autocorrelation function $g^{(2)}(t)$ was measured experimentally, which is related to normalized autocorrelation function $g^{(1)}(t)$ by the relation

$$g^{(2)}(t) = B[1 + \beta|g^{(1)}(t)|^2] \quad (3)$$

where β is a constant parameter for an optical system employed and B is a baseline term. The hydrodynamic radii of polymers were calculated from a cumulant analysis of the autocorrelation function, which was performed by fitting a polynomial up to the third order to the function $\ln(g^{(2)}(t) - 1)$. The polynomial coefficients are converted into the coefficients of the cumulant expansion of the normalized autocorrelation function

$$\ln(g^{(1)}(t)) = \ln(A) - \Gamma t + \frac{\mu_2}{2} t^2 - \frac{\mu_3}{6} t^3 \quad (4)$$

where A is the amplitude and Γ is the relaxation rate. The Γ is used to calculate the apparent diffusion coefficient, D , from the relation

$$D = (\Gamma/q^2)_{q \rightarrow 0} \quad (5)$$

where q represents the magnitude of scattering vector expressed as

$$q = \frac{4\pi n}{\lambda} \sin(\theta/2) \quad (6)$$

where n is the index of refraction of the solution. The hydrodynamic radius R_h is given by the Einstein–Stokes equation

$$R_h = \frac{k_B T}{6\pi\eta D} \quad (7)$$

where k_B is the Boltzmann constant, T is the absolute temperature, and η is the solvent viscosity. To obtain the relaxation time distribution, $\tau A(\tau)$, the inverse Laplace transform (ILT) analysis for $g^{(2)}(t)$ was performed using the algorithm REPES²⁶ according to the equation

$$g^{(1)}(t) = \tau A(\tau) \exp(-t/\tau) d \ln \tau \quad (8)$$

where τ is the relaxation time. The details of QELS instrumentation and theory are described in the literature.^{27,28}

Results and Discussion

¹H NMR Relaxation Times. Our earlier study with fluorescence labeled AMPS–DodMam copolymers made it clear that the polymers adopted an increasingly compact chain conformation as f_{Dod} was increased beyond 20 mol %.¹⁸ This conclusion was drawn mainly from fluorescence results provided by pyrene and/or naphthalene labels covalently attached to the polymers.²⁹ The compact conformation arises from hydrophobic self-association of polymer-bound dodecyl groups, leading to the formation of hydrophobic microdomains. As the hydrophobic microdomains are formed, the motional freedom of the dodecyl group will be restricted in the microdomain. Therefore, ¹H NMR relaxation times for protons in the dodecyl group may provide information about the dynamic nature of the aggregate of the polymer-bound hydrophobes.

Figure 1 depicts an example of stack plots of ¹H NMR spectra for the AMPS–DodMam copolymer with $f_{\text{Dod}} = 50$ mol % in D₂O (ionic strength was adjusted to 0.05 with NaCl) observed at 30 °C with 180°– τ –90° (Figure 1, upper) and {90°– τ (180°) τ –90°} _{n} (Figure 1, lower) pulse sequences on a 270 MHz ¹H NMR spectrometer. From these spectra the spin–lattice relaxation times (T_1) and the spin–spin relaxation times (T_2) were determined. The resonance peaks at about 0.9 and 1.3 ppm are assigned to the methyl and methylene protons in the dodecyl group, respectively. The sum of the methyl protons in the AMPS unit and the methyl and methylene protons in the main chain give an unresolved broad peak at about 1.5 ppm. Because the methyl protons in the dodecyl group give an isolated peak at about 0.9 ppm, we chose this resonance peak to determine T_1 and T_2 values.

In Figure 2, T_1 and T_2 values determined from Figure 1 are plotted against f_{Dod} . (The peak due to the methyl protons for $f_{\text{Dod}} = 10$ mol % was so small that we were unable to determine T_1 and T_2 values.) The T_1 value decreases gradually with increasing f_{Dod} up to 50 mol %, but it markedly decreases as f_{Dod} is further increased beyond 50 mol %. This indicates that the motion of the polymer-bound dodecyl groups becomes more restricted with increasing f_{Dod} up to 50 mol % because the hydrophobes form microdomains by self-association and that the motional restriction becomes more pronounced

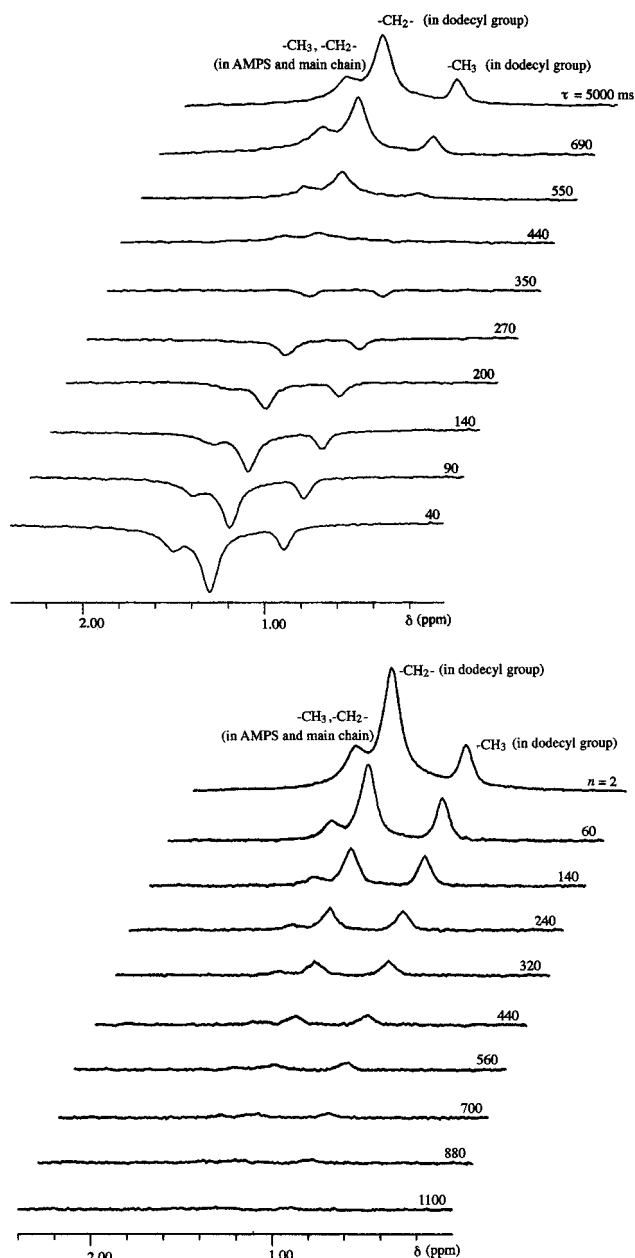


Figure 1. ¹H NMR stack plots for T_1 (upper) and T_2 (lower) measurements for the polymer with $f_{\text{Dod}} = 50$ mol % at 1 mg/mL in D₂O containing 0.05 M NaCl at 30 °C. τ and n represent the pulse interval and repeat number of the 180° pulse, respectively.

at $f_{\text{Dod}} > 50$ mol %. This observation may suggest that a conformational change occurs at $f_{\text{Dod}} \approx 50$ mol %. The spin–lattice relaxation occurs most efficiently through molecular motions whose frequency is comparable to the NMR frequency.³⁰ Therefore, T_1 decreases concurrently with T_2 as molecular motions decrease. As can be seen in Figure 2, the T_2 value decreases with increasing f_{Dod} . However, T_2 shows no such drastic change at $f_{\text{Dod}} \approx 50$ mol %. Since the T_2 is already as short as 45 ms at $f_{\text{Dod}} = 50$ mol %, T_2 may be much less sensitive to an increase in motional restriction than T_1 . It is to be noted that the motional restriction of the polymer-bound dodecyl groups does not appear to be saturated even at $f_{\text{Dod}} = 60$ mol %.

Fluorescence Depolarization. Polymer-bound naphthalene chromophores can be used as a fluorescence depolarization probe as reported by Webber and co-

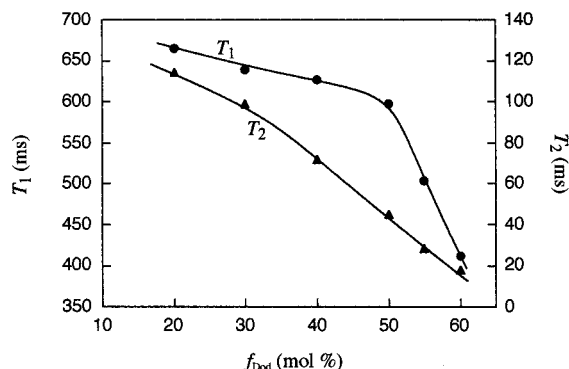


Figure 2. Plots of T_1 and T_2 for methyl protons in the polymer-bound dodecyl groups as a function of f_{Dod} measured in D_2O containing 0.05 M NaCl at 30 °C.

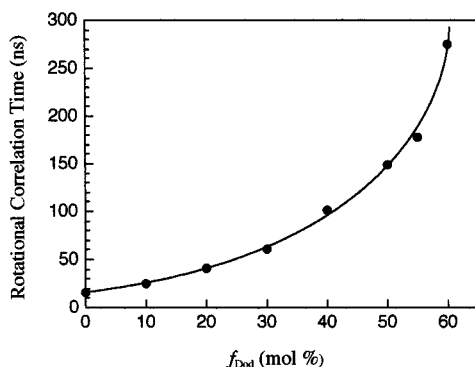


Figure 3. Rotational correlation time determined by fluorescence depolarization plotted as a function of f_{Dod} . The depolarization experiment was performed with 1 g/L polymer solutions containing 0.05 M NaCl at 25 °C.

workers.^{31,32} If naphthalene labels on AMPS–DodMAM copolymers are incorporated in hydrophobic microdomains formed by dodecyl groups, the motional restriction of the dodecyl groups may be detected by the fluorescence depolarization of the naphthalene labels. Figure 3 shows the rotational correlation time for the naphthalene label plotted as a function of f_{Dod} . The steady-state fluorescence depolarization measurements were performed with polymer solutions in 0.05 M NaCl at 25 °C, and observed anisotropy (r) values were converted into the rotational correlation times (τ_ϕ) using eq 2. With increasing f_{Dod} the τ_ϕ value increases, showing an upward curvature, over the whole range of f_{Dod} studied and does not show a tendency for saturation even at $f_{\text{Dod}} = 60$ mol %. This tendency is similar to that of ^1H NMR relaxation times.

It is important to compare the depolarization and ^1H NMR relaxation times data with other fluorescence characterization data. We previously reported that fluorescence lifetime, nonradiative energy transfer (NRET), and fluorescence quenching with thallium nitrate showed a tendency for leveling off at $f_{\text{Dod}} = 40$ –50 mol %.¹⁸ These observations suggest that, upon an increase in f_{Dod} to 40–50 mol %, the polymer chain contraction proceeds to a maximum extent and each microdomain becomes large enough to encapsulate naphthalene labels, but the tightness of the microdomain further increases with increasing f_{Dod} even at $f_{\text{Dod}} \approx 60$ mol %.

QELS. Figure 4 shows distributions of the relaxation times (τ) in QELS for the polymers with varying f_{Dod} at a polymer concentration of 1 g/L in 0.05 M NaCl aqueous solution observed at a scattering angle of 90°

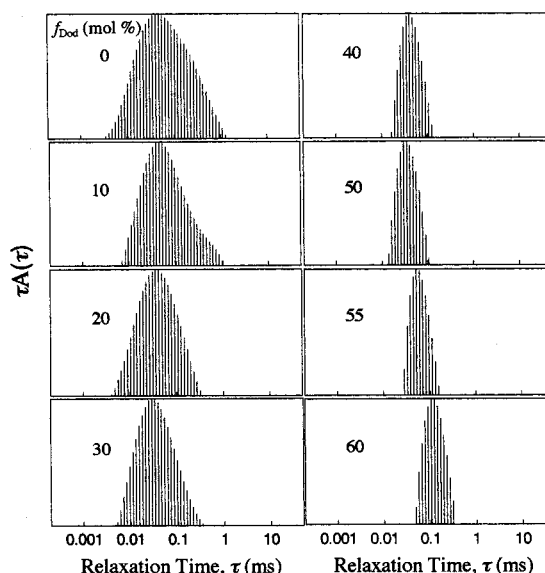


Figure 4. Distributions of the relaxation times in QELS measured at $\theta = 90^\circ$ for 1 g/L polymer solutions containing 0.05 M NaCl at 25 °C.

at 25 °C. The relaxation time distributions are unimodal except for the polymer with $f_{\text{Dod}} = 10$ mol %. In an earlier study of AMPS–DodMAM copolymers with lower contents of DodMAM, we came across the fact that some fractions of polymer chains underwent interpolymer hydrophobe associations when $f_{\text{Dod}} \leq 10$ mol %, giving a mixture of single polymer chains (i.e., unimers) and polymer aggregates.³³ The ratio of the polymer aggregate to the unimer was found to increase as the polymer concentration was increased. The relaxation time distribution was bimodal with a fast mode attributed to the unimer and a slow mode to the aggregate, the latter increasing with increasing polymer concentration.³³ The apparently bimodal distribution observed for the polymer with $f_{\text{Dod}} = 10$ mol % (Figure 4) is an indication of such interpolymer association. When f_{Dod} is increased to 20 mol %, the relaxation time distribution becomes unimodal. It is clearly seen that the distribution peak shifts toward shorter relaxation times with an increase in f_{Dod} up to 50 mol % and then begins to shift toward longer relaxation times at $f_{\text{Dod}} = 50$ mol % as f_{Dod} is further increased.

In Figure 5, relaxation rates (Γ) (i.e., $= 1/\tau$) for all the polymers (f_{Dod} ranging from 0 to 60 mol %) in 0.05 M aqueous NaCl are plotted as a function of the square of the magnitude of the scattering vector (q^2) (scattering angle ranging from 50° to 150°). Linear relationships passing through the origin observed for all the polymers imply that the measured relaxation times are attributable to a diffusive mode, allowing us to estimate a diffusion coefficient from the slope. Apparent hydrodynamic radii (R_h) were calculated from the estimated diffusion coefficients along with the viscosity and refractive index of a 0.05 M NaCl aqueous solution at 25 °C using the Stokes–Einstein relation. The results are plotted against f_{Dod} in Figure 6. As f_{Dod} is increased, R_h decreases significantly in the region $0 < f_{\text{Dod}} < 30$ mol %, reaching a minimum value of about 5 nm at $f_{\text{Dod}} = 50$ mol %. A striking observation is that R_h increases abruptly at $f_{\text{Dod}} \approx 50$ mol % as f_{Dod} is further increased. These results indicate that the hydrophobe associations of the polymer-bound dodecyl groups occur within a polymer chain in the f_{Dod} regime of 20–50 mol %, leading to the formation of unimer micelles. However,

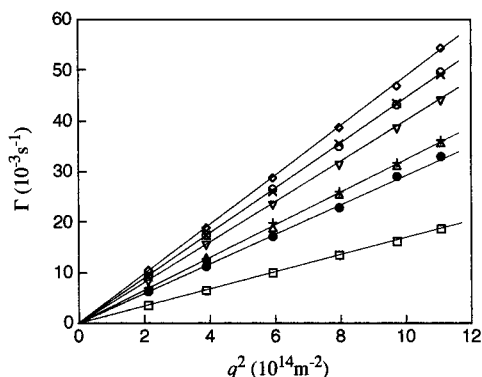


Figure 5. Plots of the relaxation rates (Γ) as a function of the square of the magnitude of the scattering vector (q^2) for the polymers with $f_{\text{Dod}} = 0$ (\bullet), 10 (Δ), 20 (∇), 30 (\circ), 40 (\times), 50 (\diamond), 55 ($+$), and 60 (\square): QELS measurements were performed in the angle range $\theta = 50^\circ$ – 150° with 1 g/L polymer solutions containing 0.05 M NaCl at 25°C .

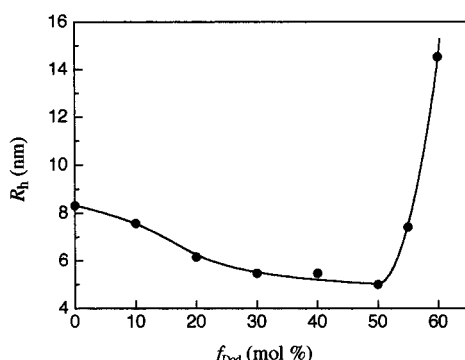


Figure 6. Plot of R_h as a function of f_{Dod} for 1 g/L polymer solutions containing 0.05 M NaCl at 25°C .

given the molecular weights of all the polymers are more or less the same (see Experimental Section), it is obvious that interpolymer associations abruptly occur when f_{Dod} is increased beyond 50 mol %.

An observation to be noted in Figure 4 is that the relaxation time distribution becomes suddenly narrower at f_{Dod} between 30 and 40 mol %, suggesting the occurrence of a drastic change in polymer conformation in this f_{Dod} regime. It should be also noted that the narrow monodisperse distributions remain as such even at $f_{\text{Dod}} \geq 55$ mol % despite the fact that interpolymer associations occur at these high f_{Dod} values. We will discuss this point in some detail in a later subsection.

Our recent studies showed that interpolymer associations of AMPS–DodMAM copolymers of low DodMAM contents (i.e., $f_{\text{Dod}} \leq 10$ mol %) were disrupted by the addition of a nonionic surfactant, *n*-dodecyl hexaoxyethylene glycol monoether (C_{12}E_6).³³ Furthermore, we found that unimer micelles of AMPS–DodMAM copolymers with $f_{\text{Dod}} = 50$ mol % were disrupted by interactions with C_{12}E_6 and form polymer–micelle complexes.³⁴ These findings imply that hydrophobic association between the polymer-bound dodecyl moiety and the surfactant is more favorable than the self-association of the polymer-bound dodecyl groups.

Relaxation time distributions for the polymers with $f_{\text{Dod}} = 55$ and 60 mol % in 0.05 M NaCl aqueous solutions monitored at a scattering angle of 90° in the absence and presence of added C_{12}E_6 at varying concentrations (ranging from 0.02 to 10 mM) are shown in Figure 7. A critical micelle concentration (cmc) and aggregation number for this surfactant are 6×10^{-5} M

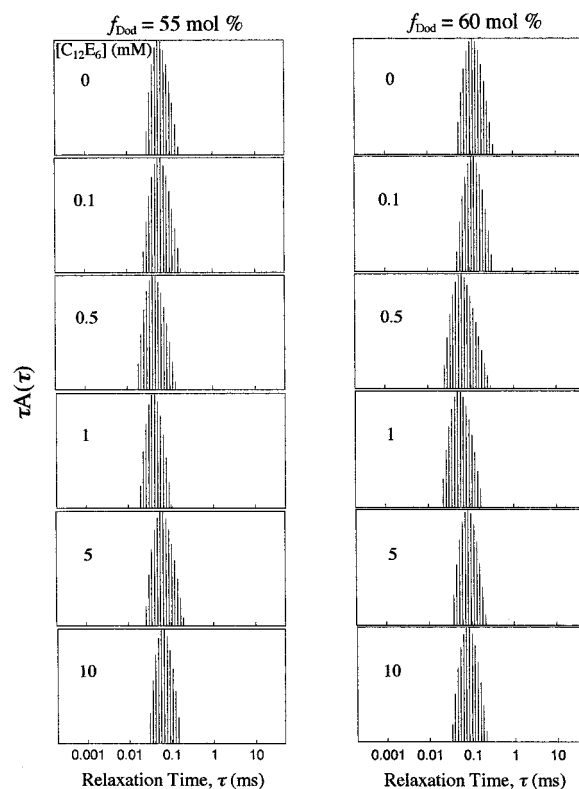


Figure 7. Relaxation time distributions in QELS at $\theta = 90^\circ$ for the polymers with $f_{\text{Dod}} = 55$ and 60 mol % at 1 g/L polymer in 0.05 M NaCl aqueous solutions in the presence of varying concentrations of C_{12}E_6 .

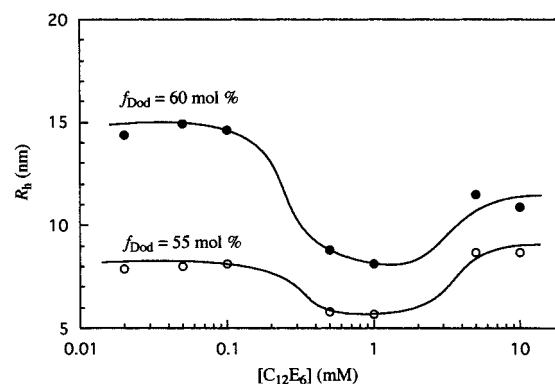


Figure 8. Plots of R_h as a function of the concentration of C_{12}E_6 for the polymers with $f_{\text{Dod}} = 55$ and 60 mol % at 1 g/L polymer in 0.05 M NaCl aqueous solutions.

and 300, respectively, at 25°C .³⁵ The relaxation time distributions remain practically the same up to a C_{12}E_6 concentration of 0.1 mM, but they shift toward shorter relaxation times at C_{12}E_6 concentrations higher than 0.5 mM and then shift back toward longer relaxation times as the C_{12}E_6 concentration is further increased up to 5 mM. Apparent R_h values were estimated from apparent diffusion coefficients obtained from Γ – q^2 plots. These R_h values are plotted against the surfactant concentration in Figure 8. The R_h values significantly decrease at a C_{12}E_6 concentration between 0.1 and 0.5 mM. This indicates that interpolymer aggregates of the polymers with $f_{\text{Dod}} = 55$ and 60 mol % are disrupted via interactions with the polymer-bound dodecyl group and C_{12}E_6 micelles, forming polymer–micelle complexes.^{33,34} When the surfactant concentration is further increased up to 5 mM, the hydrodynamic size of the polymer–micelle complex increases, arising from an increase in the

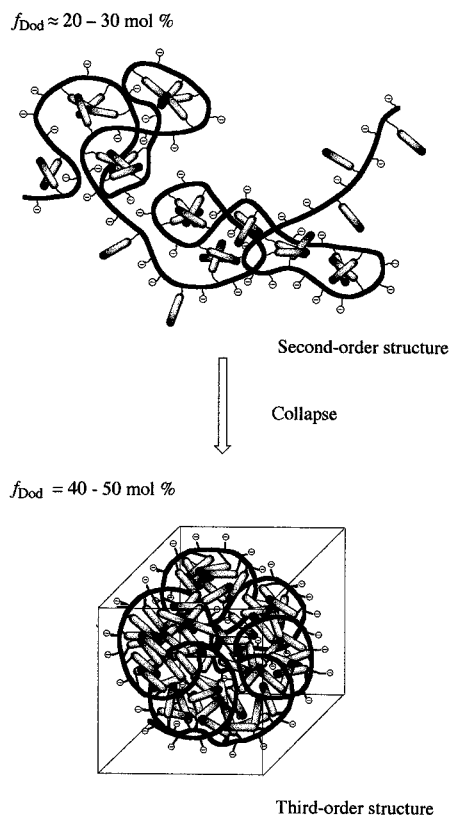


Figure 9. Conceptual illustration of hypothetical models for the two types of unimer micelles.

number of surfactant micelles bound to the polymer. These observations are an experimental manifestation for the interpolymer association for the polymers with $f_{\text{Dod}} \geq 55$ mol %.

Association Model. As we reported previously,³⁴ when $f_{\text{Dod}} \leq 10$ mol %, some polymer-bound dodecyl groups undergo interpolymer association if the polymer concentration is higher than a certain level, and thus some polymer chains are hydrophobically “cross-linked” while some polymer chains remain as unimers, the ratio of the hydrophobically cross-linked chains to the unimer chains increasing with increasing the polymer concentration. However, in the range $20 < f_{\text{Dod}} \leq 50$ mol %, intrapolymer hydrophobic association is predominant, leading to the formation of unimer micelles. A hypothetical model for the unimer micelles formed by the polymers of 20–50 mol % f_{Dod} is depicted in Figure 9. When f_{Dod} is between 20 and 30 mol %, hydrophobic microdomains are formed along the polymer chain through associations of dodecyl groups located closely within a polymer chain, and the microdomains are surrounded by charged loops. This type of micelles can be viewed as a second-order structure in which polymer chains are loosely folded. When f_{Dod} is increased to 40 mol %, however, the second-order structure is further collapsed into a third-order structure where polymer chains are highly folded. This transition from the second-order to third-order structure may correspond to the marked narrowing of the QELS relaxation time distribution (Figure 4) occurring at an f_{Dod} between 30 and 40 mol %. When f_{Dod} is further increased beyond 50 mol %, all polymer chains form interpolymer aggregates. However, the interpolymer aggregates formed at $f_{\text{Dod}} > 50$ mol % are remarkably different in nature from the interpolymer associates formed at $f_{\text{Dod}} \leq 10$ mol %. A remarkable feature for the interpolymer

aggregates formed at $f_{\text{Dod}} > 50$ mol % is that the distribution of the relaxation times in QELS is monodisperse with a narrow width (Figure 4). Moreover, the relaxation time distribution does not change at all in a wide range of polymer concentrations (0.1–10 g/L) as well as temperatures (10–70 °C) (data not shown). The structure of the interpolymer aggregates at $f_{\text{Dod}} > 50$ mol % is still an open question. A plausible model may be an aggregate of the unimer micelles of the third-order structure through associations of hydrophobic “patches” on the surface of the unimer micelle. But, we cannot rule out a possibility of a multipolymer aggregate that is formed via concurrent intra- and interpolymer hydrophobe association during the process of self-organization of the polymer.

Conclusions

Association behavior of AMPS–DodMAM copolymers in aqueous solution was studied by ¹H NMR relaxation, fluorescence depolarization, and QELS techniques, focusing on the effect of f_{Dod} on the preference of intrapolymer association and on the structure and dynamic nature of unimer micelles formed from these polymers. It was shown that the chain conformation arising from hydrophobic associations of polymer-bound dodecyl groups is a strong function of f_{Dod} . When $f_{\text{Dod}} \leq 10$ mol %, the polymers adopt relatively open chain conformation, but there is a weak tendency for interpolymer association, resulting in “hydrophobically cross-linked” chains depending on the polymer concentration. However, when f_{Dod} is in the range 20–50 mol %, intrapolymer hydrophobe associations occur predominantly, leading to the formation of unimer micelles. In the range 10–30 mol % f_{Dod} , unimer micelles with a second-order structure are formed, in which hydrophobic microdomains are formed along the polymer chain and polymer chains are loosely folded. At f_{Dod} between 30 and 40 mol %, the second-order structure is folded into a third-order structure where polymer chains are highly collapsed. At $f_{\text{Dod}} \approx 50$ mol %, unimer micelles with a highly compact third-order structure are formed. When f_{Dod} is further increased beyond 50 mol %, all polymer chains form interpolymer aggregates. However, these interpolymer aggregates are markedly different from those observed for the polymers with $f_{\text{Dod}} \leq 10$ mol % in that the size distribution is monodisperse and independent of polymer concentration. The structure of these interpolymer aggregates remains an open question.

Acknowledgment. This work was supported in part by a Grant-in-Aid for Scientific Research No. 10450354 from the Ministry of Education, Science, Sports, and Culture, Japan.

References and Notes

- (1) *Principles of Polymer Science and Technology in Cosmetics and Personal Care*; Goddard, E. D., Gruber, J. V., Eds.; Marcel Dekker: New York, 1999.
- (2) McCormick, C. L.; Bock, J.; Schulz, D. N. *Encyclopedia of Polymer Science and Engineering*; John Wiley: New York, 1989; Vol. 17, p 730.
- (3) Bock, J.; Varadaraj, R.; Schulz, D. N.; Maurer, J. J. In *Macromolecular Complexes in Chemistry and Biology*; Dubin, P., Bock, J., Davies, R. M., Schulz, D. N., Thies, C., Eds.; Springer-Verlag: Berlin, 1994; p 33.
- (4) *Polymers as Rheology Modifiers*; Schulz, D. N., Glass, J. E., Eds.; Advances in Chemistry Series 462; American Chemical Society: Washington, DC, 1991.

- (5) *Hydrophilic Polymer, Performance with Environmental Acceptability*; Glass, J. E., Ed.; Advances in Chemistry Series 248; American Chemical Society: Washington, DC, 1996.
- (6) Chang, Y.; McCormick, C. L. *Macromolecules* **1993**, *26*, 6121.
- (7) McCormick, C. L.; Chang, Y. *Macromolecules* **1994**, *27*, 2151.
- (8) Kramer, M. C.; Welch, C. G.; Steger, J. R.; McCormick, C. L. *Macromolecules* **1995**, *28*, 5248.
- (9) Hu, Y.; Kramer, M. C.; Boudreaux, C. J.; McCormick, C. L. *Macromolecules* **1995**, *28*, 7100.
- (10) Branham, K. D.; Snowden, H. S.; McCormick, C. L. *Macromolecules* **1996**, *29*, 254.
- (11) Kramer, M. C.; Steger, J. R.; Hu, Y.; McCormick, C. L. *Macromolecules* **1996**, *29*, 1992.
- (12) Hu, Y.; Smith, G. L.; Richardson, M. F.; McCormick, C. L. *Macromolecules* **1997**, *30*, 3526.
- (13) Hu, Y.; Armentrout, R. S.; McCormick, C. L. *Macromolecules* **1997**, *30*, 3538.
- (14) Morishima, Y. *Trends Polym. Sci.* **1994**, *2*, 31.
- (15) Morishima, Y.; Nomura, S.; Ikeda, T.; Seki, M.; Kamachi, M. *Macromolecules* **1995**, *28*, 2874.
- (16) Morishima, Y. In *Solvents and Self-Organization of Polymers*; Webber, S. E., Tuzar, D., Munk, P., Eds.; Kluwer Academic Publishers: Dordrecht, The Netherlands, 1996; p 331.
- (17) Morishima, Y.; Tominaga, Y.; Kamachi, M.; Okada, T.; Hirata, Y.; Mataga, N. *J. Phys. Chem.* **1991**, *95*, 6027.
- (18) Yamamoto, H.; Mizusaki, M.; Yoda, K.; Morishima, Y. *Macromolecules* **1998**, *31*, 3588.
- (19) Morishima, Y.; Kobayashi, T.; Nozakura, S. *Polym. J.* **1989**, *21*, 267.
- (20) Morishima, Y.; Tominaga, Y.; Nomura, S.; Kamachi, M. *Macromolecules* **1992**, *25*, 861.
- (21) Erdmann, K.; Gutsze, A. *Colloid Polym. Sci.* **1987**, *256*, 667.
- (22) Rady, P.; Budd, P. M.; Heatley, F.; Price, C. J. *Polym. Sci., Polym. Phys. Ed.* **1991**, *29*, 451.
- (23) Brereton, M. G.; Ward, I. M.; Boden, N.; Wright, P. *Macromolecules* **1991**, *24*, 2068.
- (24) Meiboom, S.; Gill, D. *Rev. Sci. Instrum.* **1958**, *29*, 688.
- (25) Perrin, F. *J. Phys. Radium* **1926**, *7*, 39.
- (26) Jakes, J. *Czech. J. Phys.* **1988**, *B38*, 1305.
- (27) Phillies, G. D. J. *Anal. Chem.* **1990**, *62*, 1049A.
- (28) Phillies, G. D. J. *J. Chem. Phys.* **1988**, *89*, 91.
- (29) See for example: *Photophysical and Photochemical Tools in Polymer Science*; Winnik, M. A., Ed.; Reidel: Dordrecht, The Netherlands, 1986.
- (30) Pake, G. E. In *Solid State Physics*; Seitz, F., Turnbull, D., Eds.; Academic Press: New York, 1965; Vol. 2, pp 1–92.
- (31) Kiserow, D.; Chan, J.; Ramireddy, C.; Munk, P.; Webber, S. E. *Macromolecules* **1992**, *25*, 5338.
- (32) Chan, J.; Fox, S.; Kiserow, D.; Ramireddy, C.; Munk, P.; Webber, S. E. *Macromolecules* **1993**, *26*, 7016.
- (33) Hashizdume, A.; Yamamoto, H.; Mizusaki, M.; Morishima, Y. *Polym. J.*, in press.
- (34) Hashizdume, A.; Mizusaki, M.; Yoda, K.; Morishima, Y. *Langmuir* **1999**, *15*, 4276.
- (35) Lianos, P.; Zana, R. *J. Colloid Interface Sci.* **1981**, *84*, 100.

MA9907791